Light-scattering resonances in small spheres

Gorden Videen and William S. Bickel
Physics Department, University of Arizona, Tucson, Arizona 85721
(Received 24 October 1991)

Two limiting expressions occur for scattering from very small spheres. One occurs when the refractive index becomes small (Rayleigh scattering), and the other occurs when the sphere becomes perfectly conducting (Thomson scattering). We explore the scatter from small spheres having real refractive indices. For such spheres, resonance conditions occur, and the resulting scattering coefficients are no longer proportional to the volume of a sphere.

PACS number(s): 42.25.Fx

INTRODUCTION

Electromagnetic scattering from small spheres was explored by Rayleigh [1] and Thomson [2], who calculated light-scattering expressions for two very different special cases: where the spheres have small refractive indices, and where they are perfect conductors, respectively. They did this before Mie [3] and Lorenz [4] derived a formalism for the scatter from arbitrary spheres. The range of validity of these special limits has been explored by Kerker, Scheiner, and Cooke [5]. They found that as the sphere size becomes smaller, Rayleigh theory is valid over a larger range of refractive index, and Thomson theory is valid over a smaller range of refractive index.

We might expect the scattering that occurs from small spheres that lie in the region between the Rayleigh and the Thomson limits to be composed of some combination of the modes present at these two limits. However, the extinction efficiencies of small, dielectric spheres as a function of refractive index (Fig. 1) are not smooth, but complicated by sharp resonances. Resonances in the light scattering from spheres have attracted a great deal of attention recently [6–16]. Resonances appear as strong, narrow enhancements in the scattering of a particle. The large internal fields that are built up within such particles can create interesting effects and have been used to investigate various phenomena such as fluorescent and Raman scattering [17–24].

It is well known that as the sphere size becomes small with respect to the illuminating wavelength, the equations predicting the scatter are greatly simplified, since only a few sets of coefficients are necessary to characterize the scatter. We take advantage of these simplified expressions and derive the resonance conditions directly from the a_n and b_n coefficients [25–27] rather than from the A_n, B_n, C_n, D_n coefficients [28], which is the standard method. We then explore the scattering behavior and cross sections on and near resonance. Studying resonances in small spheres gives insight into the resonances that occur in larger spheres and even in more complicated particles.

We note that the resonance conditions in these small spheres are met when the sphere refractive index is large ($m > \pi/x$). Therefore, it would seem that this work would constitute only a theoretical exercise, which could only provide insight into other resonance situations. However, in a recent paper, Scully [29] has shown via quantum coherence that when operating near an atomic resonance between an excited state and a coherently prepared ground-state doublet, a large enhancement of the refractive index (by many orders of magnitude) may be achieved with zero absorption. In this case, the light-scattering resonances that we examine cannot only be realized, but may prove to be a useful tool in characterizing the optical properties of such materials.

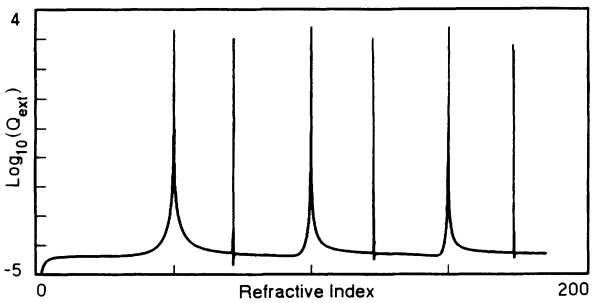

FIG. 1. Extinction efficiency for a small ($r = 0.01\lambda$) sphere as a function of real refractive index.

SCATTERING COEFFICIENTS

The electromagnetic scattering a large distance from a sphere of radius r, illuminated by a unit-normalized plane wave traveling in the positive z direction, and polarized in the $\hat{\mathbf{x}}$ direction, may be expressed by two scattering amplitude functions given by

$$S_1 = \sum_{n=1}^{\infty} \frac{2n+1}{n(n+1)} \left[\frac{P_n^1(\cos\vartheta)}{\sin\vartheta} a_n + \frac{\partial}{\partial\vartheta} P_n^1(\cos\vartheta) b_n \right], \tag{1a}$$

$$S_2 = \sum_{n=1}^{\infty} \frac{2n+1}{n(n+1)} \left[\frac{P_n^1(\cos\vartheta)}{\sin\vartheta} b_n + \frac{\partial}{\partial\vartheta} P_n^1(\cos\vartheta) a_n \right], \tag{1b}$$

where S_1 is measured in the y-z plane and S_2 is measured in the x-z plane. The Mie scattering coefficients are given by

$$a_n=\frac{m\psi_n'(x)\psi_n(mx)-\psi_n'(mx)\psi_n(x)}{m\xi_n'(x)\psi_n(mx)-\psi_n'(mx)\xi_n(x)}\ , \tag{2a}$$

$$b_n=\frac{m\psi_n'(mx)\psi_n(x)-\psi_n'(x)\psi_n(mx)}{m\psi_n'(mx)\xi_n(x)-\xi_n'(x)\psi_n(mx)}\ , \tag{2b}$$

where m is the complex refractive index of the sphere, $x=2\pi r/\lambda$, and ψ_n and ξ_n are the Riccati-Bessel functions.

First we examine what happens for the special limiting case where the sphere size is small ($r\ll\lambda$). In this limiting case the scatter is determined primarily by the lowest-order terms of the series given by Eq. (1). The Riccati-Bessel functions for the $n=1$ case are given by

$$\psi_1(\rho)=\frac{\sin\rho}{\rho}-\cos\rho\ ,\quad \xi_1(\rho)=\exp(i\rho)(-i\rho^{-1}-1)\ . \tag{3}$$

For small arguments, these functions are approximately

$$\psi_1(\rho)\sim\frac{\rho^2}{3}-\frac{\rho^4}{30}\ ,\quad \xi_1(\rho)\sim-\frac{i}{\rho}-\frac{i\rho}{2}+\frac{\rho^2}{3}\ . \tag{4}$$

For small x, the scattering coefficients given by Eq. (2) are approximately

$$a_1\sim\frac{\cos(mx)\left[x\left[\frac{1+2m^2}{3m}\right]-x^3\left[\frac{1+4m^2}{30m}\right]\right]+\sin(mx)\left[-\left[\frac{1+2m^2}{3m^2}\right]+x^2\left[\frac{1+14m^2}{30m^2}\right]\right]}{\cos(mx)\left[x^{-2}\left[\frac{-i+im^2}{m}\right]-\left[\frac{i+im^2}{2m}\right]\right]+\sin(mx)\left[x^{-3}\left[\frac{i-im^2}{m^2}\right]+x^{-1}\left[\frac{i-im^2}{2m^2}\right]\right]}\ ,$$

$$b_1\sim\frac{\cos(mx)(x-x^3/6)+\sin(mx)\left[-1/m+x^2\left[\frac{1+2m^2}{6m}\right]\right]}{\cos(mx)(-i+x)+\sin(mx)\left[x^{-1}\left[\frac{i-im^2}{m}\right]-1/m-x\left[\frac{i+im^2}{2m}\right]\right]}\ . \tag{5}$$

Similarly, the second-order coefficients may be written as in Eq. (6).

Two additional limiting conditions exist for small spheres. One is the Rayleigh limit valid when $|m|x\ll 1$. In this case the scattering coefficients further reduce to

$$a_1\sim-\frac{2ix^3}{3}\frac{m^2-1}{m^2+2}\ ,\quad b_1\sim 0\ ,$$
$$a_n\sim b_n\sim 0\ \text{ for } n>1\ . \tag{7}$$

The other limiting condition occurs when the sphere's refractive index approaches that of a perfect conductor $m\to i\infty$. In this case the scattering coefficients reduce to

$$a_1\sim-\frac{2ix^3}{3}\ ,\quad b_1\sim\frac{ix^3}{3}\ ,$$
$$a_n\sim b_n\sim 0\ \text{ for } n>1\ . \tag{8}$$

Note that in both these limiting cases the scattering coefficients are proportional to x^3. Figure 2 shows the angular scattering-intensity distributions for a Rayleigh and a Thomson sphere.

RESONANCES

We now examine the b_1 mode in more detail. When the refractive index m is increased along the real axis, the sine terms in Eq. (5) do not contribute to the scatter when $mx=N\pi$ where the index N is an integer. Resonances in the b_1 coefficients occur at approximately these locations. Two interesting results occur that are worth pointing out. The first is that the scattered fields are no longer proportional to the sphere volume. As a result, the scattering efficiencies of such particles are greatly increased compared to particles just off resonance. Figure 3 shows the first b_1 resonance (following a previous convention [8]; this is written as b_1^1). For purposes of illustration, we chose to examine small spheres with an arbitrary but definite radius $r=0.01\lambda$. The resulting resonances will necessarily occur only at large values of refractive index ($m=50N$) due to the small size of these spheres.

The second interesting result is that the mode of oscil-

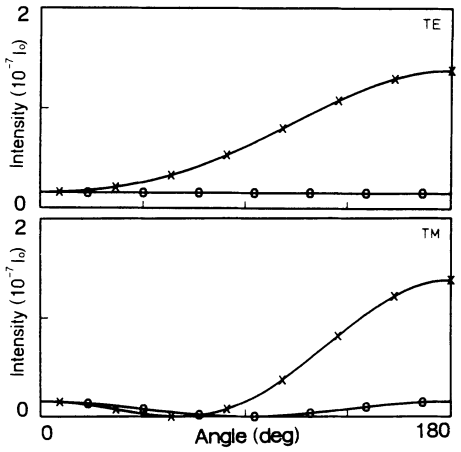

FIG. 2. Angular scattering-intensity distributions for an $r=0.01\lambda$, $m=2.0$ Rayleigh sphere (○), and an $r=0.01\lambda$ Thomson sphere (×).

$$a_2 \sim \frac{\cos(mx)\left[-x\left[\frac{2+3m^2}{5m^2}\right]+x^3\left[\frac{6+29m^2}{210m^2}\right]\right]+\sin(mx)\left[\left[\frac{2+3m^2}{5m^3}\right]-x^2\left[\frac{2+19m^2+14m^4}{70m^3}\right]\right]}{\cos(mx)\left[x^{-4}\left[\frac{18i-18im^2}{m^2}\right]+x^{-2}\left[\frac{3i-3im^2}{m^2}\right]\right]+\sin(mx)\left[x^{-5}\left[\frac{18i-18im^2}{-m^3}\right]+x^{-3}\left[\frac{-3i+9im^2-6im^4}{m^3}\right]\right]},$$

$$b_2 \sim \frac{\cos(mx)\left[-x/m+x^3\left[\frac{3+2m^2}{30m}\right]\right]+\sin(mx)\left[1/m^2-x^2\left[\frac{1+4m^2}{10m^2}\right]\right]}{\cos(mx)\left[x^{-2}\left[\frac{3i-3im^2}{m}\right]+\left[\frac{3i-im^2}{2m}\right]\right]+\sin(mx)\left[x^{-3}\left[\frac{3im^2-3i}{m^2}\right]+x^{-1}\left[\frac{3im^2-3i}{2m^2}\right]\right]}, \quad (6)$$

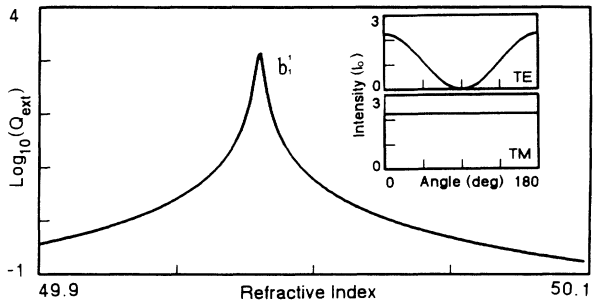

FIG. 3. Extinction efficiency for a small ($r=0.01\lambda$) sphere as a function of real refractive index near the b_1^1 resonance. Also shown are the scattering intensities for the TE and TM modes on the b_1^1 resonance ($m=49.980\,06$).

lation for the resonant sphere (b_1) is completely different than that for the Rayleigh sphere (a_1). The resulting field distributions (also shown in Fig. 3) for the b_1-resonant sphere will necessarily be different from the Rayleigh sphere (shown in Fig. 2). The TE and TM Rayleigh-sphere intensities are proportional to the TM and TE b_1-resonant sphere intensities, respectively. For the b_1 mode, the incident electromagnetic field induces a dipole moment *perpendicular* to the incident electric field.

The b_1 resonances do not account for all the resonances shown in Fig. 1. Resonances in the a_1 and b_2 modes occur when $\tan(mx)$ is approximately equal to mx [for large mx, this occurs approximately when $mx \sim (N+\frac{1}{2})\pi$]. The a_1^1 and b_2^1 resonances are shown in Fig. 4. These resonances are much narrower [half-width of the order $\Delta(mx)/(mx) \sim 10^{-7}$] than the b_1^1 resonances [half-width of the order $\Delta(mx)/(mx) \sim 10^{-5}$]. Resonances in the higher-order modes are not as prominent, since the resonant fields are proportional to x^k where $k \geq 3$.

Equations (5) and (6) not only can be used to predict where resonances occur, but can also provide information on the shapes of the resonances. We will now take a closer look at the b_1 resonance. If we express the complex refractive index as $m=m_r+im_i$, where m_r and m_i are both real quantities, we can expand the sine and cosine function about the resonance locations,

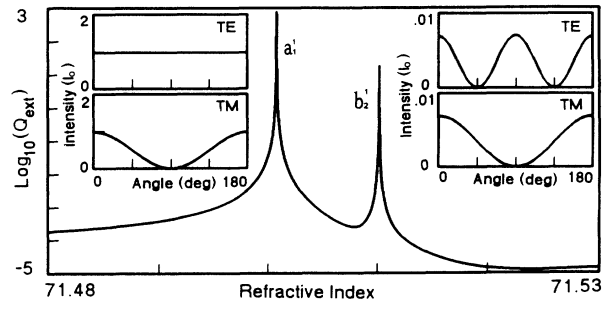

FIG. 4. Extinction efficiency for a small ($r=0.01\lambda$) sphere as a function of real refractive index near the a_1^1 and b_2^1 resonances. Also shown are the scattering intensities for the TE and TM modes on the a_1^1 ($m=71.500\,79$) and b_2^1 resonances ($m=71.510\,15$).

$$\sin(mx)=(-1)^N\sin(mx-N\pi)$$
$$\sim(-1)^N[i\sinh(m_i x)+\Delta\cosh(m_i x)]\ ,$$
$$\cos(mx)=(-1)^N\cos(mx-N\pi)$$
$$\sim(-1)^N[\cosh(m_i x)-i\Delta\sinh(m_i x)]\ , \tag{9}$$

where $m_r x\sim N\pi$, and $\Delta=m_r x-N\pi$.

Near resonance, the scattering coefficient b_1 can be simplified:

$$b_1\sim\frac{\left[x\cosh(m_i x)+i\left[\frac{x^2 m}{3}-\frac{1}{m}\right]\sinh(m_i x)\right]}{\frac{m}{x}\sinh(m_i x)-i\cosh(m_i x)}\times\frac{1}{1+\Delta/\bar{\Delta}}\ ,$$

$$\text{where } \bar{\Delta}=\frac{(x^2-ix)\cosh(m_i x)+m\sinh(m_i x)}{-im\cosh(m_i x)}\ . \tag{10}$$

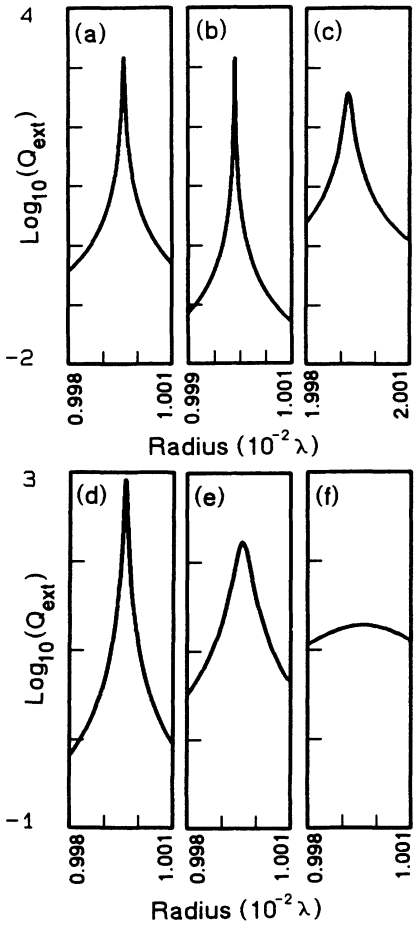

FIG. 5. Extinction efficiency near the b_1 resonances: (a) for an $m=50.0$ sphere where $N=1$; (b) for an $m=100.0$ sphere where $N=2$; (c) for an $m=50.0$ sphere where $N=2$; (d) for an $m=50.0+0.01i$ sphere where $N=1$; (e) for an $m=50.0+0.01i$ sphere where $N=1$; and (f) for an $m=50.0+0.1i$ sphere $N=1$. Radius $r=0.01\lambda$.

Equation (10) may be simplified if we assume the absorption is small ($m_i x\ll 1$),

$$b_1\sim\frac{x}{x+mm_i}\frac{1}{1+\frac{(\Delta+x/m)}{ix^2/m+im_i x}}\ . \tag{11}$$

Multiplying Eq. (11) by its complex conjugate yields a Lorentzian function centered at $\Delta=-x/m$, with a half-width of $x^2/m+m_i x$. We note that as the absorption is increased from zero, the amplitude of b_1 will decrease, and the half-width will increase. When $mm_i\gg x$, the amplitude will be proportional to $1/m_i$ and the half-width will be proportional to m_i. These dependencies were reached empirically for larger spheres having moderate refractive indices [9]. This type of analysis may also be performed for the a_1 and b_2 resonances.

The dependence of the line shapes on the size and refractive index is shown in Fig. 5. In Fig. 5(a), the $m=50.0$ sphere passes through the b_1^1 resonance as its radius is increased. In Figs. 5(b) and 5(c), we can examine the b_1^2 resonances as the radius of an $m=100.0$ sphere and an $m=50.0$ sphere is increased, respectively. Going to a higher index by increasing the refractive index [Fig. 5(b)] results in a narrower resonance. Going to a higher index by increasing the size parameter [Fig. 5(c)] results in a broader resonance. The latter result has been discussed previously for spheres much larger than the wavelength [7,10,11]. Figure 5 also shows the shape and the width of the b_1^1 resonance as the refractive index is changed from $m=50.0+0.001i$ [Fig. 5(b)] to

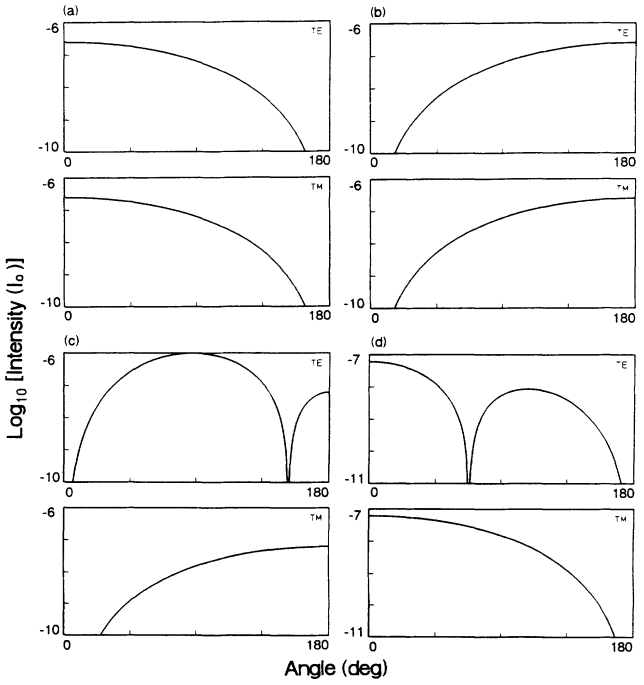

FIG. 6. Angular scattering-intensity distributions for a small ($r=0.01\lambda$) sphere having refractive indices: (a) $m=43.666\,10$, (b) $m=59.226\,10$, (c) $m=71.508\,44$, and (d) $m=71.519\,92$.

$m=50.0+0.01i$ [Fig. 5(e)] to $m=50.0+0.1i$ [Fig. 5(f)]. These figures verify that increasing the imaginary part of the refractive index results in a reduction of the height and an increase in the width of the resonant peak. This conclusion has also been discussed when examining large spheres [7–9,13].

The angular intensity distributions for spheres having refractive indices between resonant values do not necessarily resemble the distributions of either a Rayleigh or a Thomson sphere. Figure 6 shows that cases exist when the forward scatter ($\vartheta \sim 0°$) is down several orders of magnitude [in cases of Figs. 6(b) and 6(c), $a_1+b_1+5b_2/3 \sim 0$] and when the backscatter ($\vartheta \sim 180°$) is down several orders of magnitude [in cases of Figs. 6(a) and 6(d), $a_1-b_1+5b_2/3 \sim 0$]. These are important points because most scattering studies of spheres would lead one to believe that the intensity in the forward-scattering or backscattering directions would not extend several orders of magnitude below the scattered intensity at other scattering angles.

SUMMARY

For the limiting case when sphere size is much smaller than the incident wavelength, the equations describing the scatter are greatly simplified. When two additional limiting conditions on the refractive index are applied, these equations are simplified further. When the refractive index is increased along the real axis, resonance conditions develop that complicate the resulting scatter. Precisely because these resonances occur, no limiting condition can be reached as the complex refractive index is increased along the real axis. Resonances have been studied extensively for large spheres. Studying the resonances in smaller spheres in which the equations are greatly simplified gives insight to the resonance behavior occurring in larger spheres.

ACKNOWLEDGMENTS

This research was supported in part by the U.S. Air Force Office at Scientific Research (AFSC), the Petroleum Research Fund (PRF) and the Itek Corporation.

[1] Lord Rayleigh, Philos. Mag. **41**, 107 (1871); **41**, 274 (1871); **41**, 447 (1871).

[2] J. J. Thomson, *Recent Researches in Electricity and Magnetism* (Oxford University Press, London, 1893).

[3] G. Mie, Ann. Phys. (Leipzig) **25**, 377 (1908).

[4] L. Lorenz, *Oeuvres Scientifiques* (Johnson, New York, 1964).

[5] M. Kerker, P. Scheiner, and D. D. Cooke, J. Opt. Soc. Am. **68**, 135 (1978).

[6] P. Chýlek, J. Opt. Soc. Am. **66**, 285 (1976).

[7] P. Chýlek, J. T. Kiehl, and M. K. W. Ko, Phys. Rev. A **18**, 2229 (1978).

[8] P. Chýlek, J. T. Kiehl, and M. K. W. Ko, Appl. Opt. **17**, 3019 (1978).

[9] H. S. Bennett and G. J. Rosasco, Appl. Opt. **17**, 491 (1978).

[10] P. R. Conwell, P. W. Barber, and C. K. Rushforth, J. Opt. Soc. Am. A **1**, 62 (1984).

[11] J. R. Probert-Jones, J. Opt. Soc. Am. A **1**, 822 (1984).

[12] P. Chýlek, J. D. Pendleton, and R. G. Pinnick, Appl. Opt. **24**, 3940 (1985).

[13] B. A. Hunter, M. A. Box, and B. Maier, J. Opt. Soc. Am. A **5**, 1281 (1988).

[14] P. Chýlek and J. Zhan, J. Opt. Soc. Am. A **6**, 1846 (1989).

[15] P. Chýlek, J. Opt. Soc. Am. A **7**, 1609 (1990).

[16] J. A. Lock, Appl. Opt. **29**, 3180 (1990).

[17] A. Ashkin and J. M. Dziedzic, Phys. Rev. Lett. **38**, 1351 (1977).

[18] R. E. Benner, P. W. Barber, J. F. Owen, and R. K. Chang, Phys. Rev. Lett. **44**, 475 (1980).

[19] A. Ashkin and J. M. Dziedzic, Appl. Opt. **20**, 1803 (1981).

[20] J. F. Owen, P. W. Barber, P. B. Dorain, and R. K. Chang, Phys. Rev. Lett. **47**, 1075 (1981).

[21] R. Thurn and W. Kiefer, Appl. Opt. **24**, 1515 (1985).

[22] J. B. Snow, S.-X. Qian, and R. K. Chang, Opt. Lett. **10**, 37 (1985).

[23] R. G. Pinnick, A. Biswas, P. Chýlek, R. Armstrong, H. Latifi, E. Greegan, V. Srivastava, M. Jarzembski, and G. Fernandez, Opt. Lett. **13**, 494 (1988).

[24] P. Chýlek, A. Biswas, M. Jarzembski, V. Srivastava, and R. Pinnick, Appl. Phys. Lett. **52**, 1642 (1988).

[25] H. C. van de Hulst, *Light Scattering by Small Particles* (Dover, New York, 1981).

[26] M. Kerker, *The Scattering of Light and Other Electromagnetic Radiation* (Academic, New York, 1969).

[27] C. Bohren and D. Huffman, *Absorption and Scattering of Light by Small Particles* (Wiley, New York, 1983).

[28] P. Chýlek, J. Opt. Soc. Am. **63**, 699 (1973).

[29] M. O. Scully, Phys. Rev. Lett. **67**, 1855 (1991).